Dithienosilolothiophene, a new polyfused donor for organic electronics

Bob C. Schroeder,[a, b, *] *Mindaugas Kirkus,*[a,c] *Christian B. Nielsen,*[a] *Raja Shahid Ashraf,*[a] *and Iain McCulloch* [a,c]

[a] Department of Chemistry and Centre for Plastic Electronics, Imperial College London, London, SW7 2AZ, United Kingdom.

[b] Current Address: Department of Chemical Engineering, Stanford University, 443 Via Ortega, Stanford, California 94305, United States.

[c] Physical Sciences and Engineering Division, King Abdullah University of Science and Technology (KAUST), Thuwal, Saudi Arabia.

We report the synthesis of a novel pentacyclic donor moiety, dithienosilolothiophene, and its incorporation into low bandgap semiconducting polymers. The unique geometry of this new donor allowed attaching four solubilising side chains on the same side of the fused ring system, thus ensuring sufficient solubility when incorporated into conjugated polymers while simultaneously reducing the steric hindrance between adjacent polymer chains. The opto-electronic properties of three new polymers comprising the novel pentacyclic donor were investigated and compared to structurally similar thieno[3,2-*b*]thienobis(silolothiophene) polymers. Organic solar cells were fabricated in order to

evaluate the new materials' potential as donor polymers in bulk heterojunction solar cells and gain further insight into how the single sided side chain arrangement affects the active layer blend morphology.

INTRODUCTION

A lot of focus in recent years has been to develop fused building blocks, like benzodithiophene (BDT),[1, 2] benzotrithiophene (BTT) [3, 4] or indacenodithiophene (IDT) derivatives.[5, 6] By fusing the aromatic rings, the conformational disorder along the polymer backbone can be significantly reduced, in comparison to thiophene based polymers, thus potentially allowing better charge transport along the polymer backbone and stronger interchain π-π stacking interactions. Previously we reported the synthesis of a new electron rich hexacyclic donor unit, thieno[3,2-*b*]thienobis(silolothiophene) (**Si4T**) and demonstrated its potential as a building block in donor polymers for polymer:fullerene bulk-heterojunction (BHJ) solar cells.[7] One potential drawback of the **Si4T** design is the side-chain arrangement along the polymer backbone. The both-sided decoration of the conjugated backbone with solubilising alkyl side-chains promotes undoubtedly the excellent solubility of the material, however it could also hinder charge separation at the donor-acceptor interface by increasing the spatial separation between the polymer backbone and the fullerene acceptor. Graham *et al.* suggested that the fullerene acceptor preferentially docks to the electron accepting moiety of the conjugated polymer and that this part of the polymer backbone should not be sterically obstructed.[8] A good orbital overlap between the conjugated polymer backbone and the fullerene acceptor is essential to facilitate the exciton dissociation, thus yielding higher short-circuit currents (J_{sc}) in polymer-fullerene solar cells.[9, 10] One possibility of increasing the orbital overlap would be

to reduce the steric hindrance caused by the alkyl side-chains. However a shortening of the side-chains often leads to significantly reduced solubility, making the processing of the polymer unnecessarily difficult. An alternative and less explored possibility is to attach the alkyl side-chains only on one side of the polyfused donor moiety, instead of both sides. This approach liberates one side of the conjugated unit from bulky side-chains, creating sterically available approach from either another sterically free polymer backbone, or fullerene molecule and potentially would allow for a more efficient charge transfer between donor polymer and acceptor fullerene.

In this paper we present the synthesis of a new pentacyclic dithienosilolothiophene donor unit on which the four solubilising side chains are attached on the same side of the fused ring system. We investigate how this structural modification affects the spectroscopic and solid state properties of the material and ultimately the power conversion efficiency (PCE) of organic solar cells when incorporated into donor polymers.

RESULTS AND DISCUSSION

Initially we were aiming to synthesize target monomer **6** via a similar route we used for our previously published synthesis of thieno[3,2-*b*]thienobis(silolothiophene) (**Si4T**).[7] However, problems were encountered during the palladium catalysed Negishi coupling between (3-bromothiophen-2-yl)zinc(II) chloride (**2**) and 3,4-dibromo-2,5-diiodothiophene. Several reaction conditions were tested using various palladium catalysts, reaction solvents, times and temperatures, but each time, complex reaction mixtures with a significant amount of deiodated thiophene derivatives were recovered. Therefore, we adapted our approach and synthesized the tetrabrominated terthiophene intermediate (**3**)

following the literature procedure published by Mitsudo *et al*.[11] The synthetic pathway towards the novel distannylated dithienosilolothiophene (**6**) monomer is outlined in Scheme 1.

Scheme 1. Synthetic pathway towards the dithienosilolothiophene monomer (6).

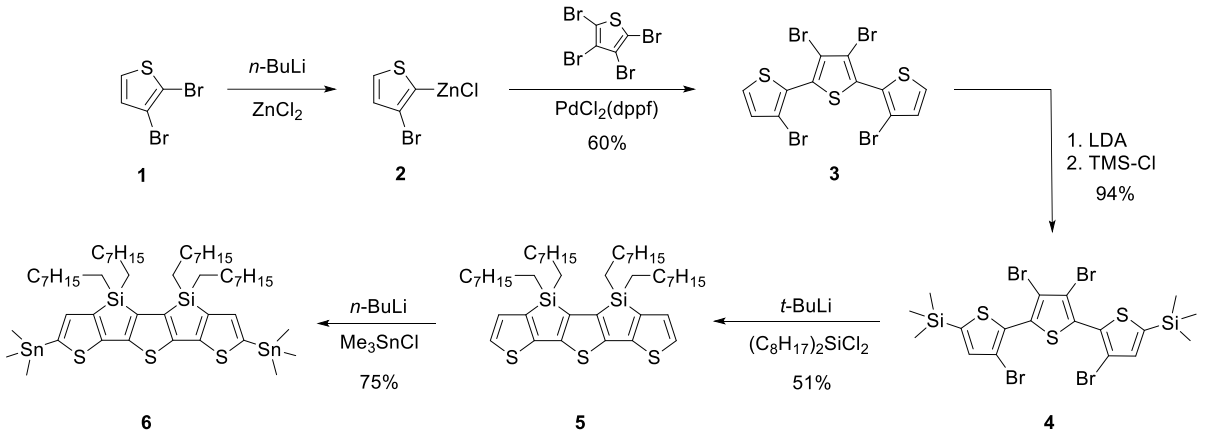

High selectivity for the α-positions of tetrabromothiophene was achieved when [1,1′-bis(diphenylphosphino)ferrocene]dichloro- palladium (II) was used as catalyst and the tetrabrominated terthiophene moiety (**3**) was successfully isolated in good yield. To prevent side-reactions during the subsequent ring-closing reaction, the α-positions were protected with trimethylsilyl groups. The terthiophene derivative (**4**) was successfully lithiated by employing *tert*-butyllithium and after quenching the tetralithiated intermediate by the addition of 2.2 equivalents of di-*n*-octyldichlorosilane, the ring-closed dithienosilolothiophene (**5**) was obtained. The double ring-closure proceeded in exceptionally high yields, which was unexpected for such an entropically unfavoured reaction step and even more so considering the much lower yields we previously obtained during the synthesis of similar polyfused heteroacenes.[12] In order to incorporate the new

donor unit into semiconducting polymers the terminal 2 and 7 positions were functionalized with trimethylstannyl groups.

Scheme 2. Chemical structures of the synthesized **Si3T** containing polymers.

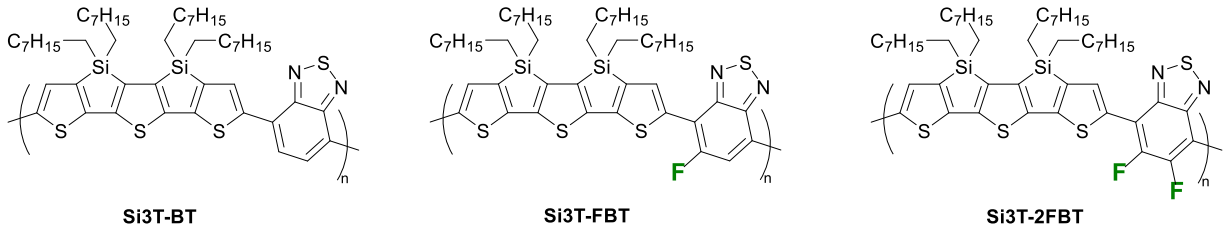

To investigate the potential of the new pentacyclic donor unit and to compare it to the previously published polyfused thieno[3,2-*b*]thienobis(silolothiophene) (**Si4T**) unit, three different low-bandgap polymers were prepared via Stille polycondensation. Given the electron rich character of the dithienosilolothiophene, rather high HOMO energy levels could be expected for the final polymers. To counterbalance this and to ensure sufficiently high open-circuit voltages (V_{oc}) in bulk-heterojunction solar cells, **Si3T** monomer **6** was co-polymerized with strong acceptor units, 4,7-dibromobenzo[*c*][1,2,5]thiadiazole (**BT**), 4,7-dibromo-5-fluorobenzo[*c*][1,2,5]thiadiazole (**FBT**) and 4,7-dibromo-5,6-difluorobenzo[*c*][1,2,5]thiadiazole (**2FBT**). All three polymer structures are depicted in Scheme 2. Even though **Si3T-FBT** is represented in Scheme 2 as regioregular, we would like to emphasize that no additional precautions were taken to counter the non-centrosymmetric nature of the **FBT** monomer and it has to be assumed therefore that the **Si3T-FBT** polymer is regiorandom in nature. The crude polymers were endcapped and purified by Soxhlet extractions in methanol, acetone, hexane and chloroform. Residual palladium was chelated with sodium diethyldithiocarbamate and extracted from the organic

polymer solution via aqueous wash.[13] The purified polymers were recovered as dark blue solids after precipitation into methanol. All three polymers were recovered with comparable molecular weights and narrow dispersities (Table 1), whilst still maintaining excellent solubility in common organic solvents due to the four octyl side-chains per repeating unit.

Table 1. Molecular weights of the **Si3T** polymers.

Polymer	M_n [a] [kg/mol]	M_w [b] [kg/mol]	Đ [c]
Si3T-BT	11	15	1.4
Si3T-FBT	13	18	1.4
Si3T-2FBT	18	26	1.4

[a] Number-average molecular weight. [b] Weight-average molecular weight. [c] Weight dispersity defined as M_w/M_n.

UV-vis. absorption spectra of all polymers were recorded in chlorobenzene solution and in thin films deposited via spin-coating from chlorobenzene solution (Figure 2, Table 2). The three polymers show broad and intense intramolecular charge-transfer (ICT) bands at lower energies (550-800 nm) and less intense absorption feature at higher energies (400-500 nm) originating from π-π* transitions.

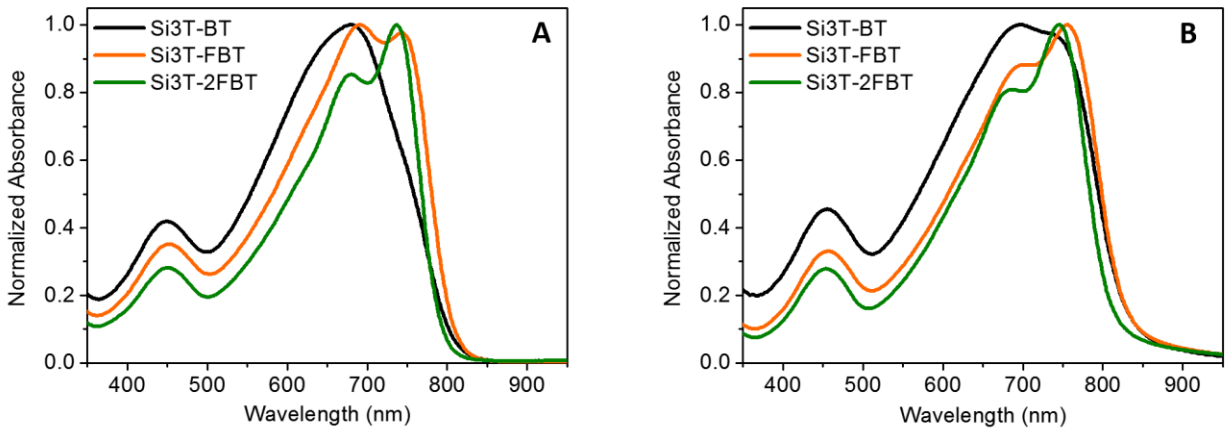

Figure 2. Normalized optical absorption spectra of **Si3T** polymers in dilute chlorobenzene (CB) solution (**A**) and as thin films spin-casted from CB solution (**B**).

At closer inspection however, several differences between the various absorption spectra become apparent. Whereas **Si3T-BT** presents only a broad ICT absorption band with a maximum at 678 nm, the ICT band of both fluorinated polymers possesses more defined features with two absorption maxima. The absorption maximum for **Si3T-FBT** is at 691 nm and a second, slightly weaker in intensity maximum is found at 740 nm. The two absorption maxima of **Si3T-2FBT** at 680 and 737 nm however follow the opposite trend and it is the higher wavelength peak that is more intense. It has previously been shown, that the sulfur's lone pairs on the donor unit and the electronegative fluorine substituents on the benzothiadiazole unit exhibit attractive interactions leading to short, non-covalent contacts, thus reducing the rotational freedom and stiffening the polymer backbone.[14-16] As a consequence, the additional peaks observed in the absorption spectra in solution of **Si3T-FBT** and **Si3T-2FBT** are likely to be caused by polymer chain aggregation. To verify this hypothesis, the absorption spectra of each polymer were taken at different concentrations (Figure S4 to S6). In both cases, the high wavelength absorption maxima decrease with

increasing dilution, thus confirming that this peak originates from polymer aggregates. Interestingly, the decrease of the aggregation peak in **Si3T-FBT** is much more dramatic than for **Si3T-2FBT**, thus suggesting that the presence of one additional fluorine atom on **2FBT** leads to a more significant reduction of rotational freedom along the polymer backbone, which encourages polymer aggregation. Furthermore it has to be taken into account that **FBT** is a non-centrosymmetric moiety and that its regiorandom incorporation into the polymer backbone will induce conformational disorder along the polymer chain. All thin film UV-vis. absorption spectra are bathochromically shifted compared to the solution spectra, with the most significant shifts observed for **Si3T-BT** and **Si3T-FBT**. The overall shape of the absorption bands of **Si3T-BT** and **Si3T-2FBT** in the solid state does not change dramatically compared to the absorption spectra in solution. In case of the mono-fluorinated polymer **Si3T-FBT** however, the second very distinctive absorption feature observed at 691 nm in the solution spectrum is only present as a low-wavelength shoulder in the solid state spectrum.

Cyclic voltammetry performed on polymer films on indium tin oxide (ITO) substrates, was used to determine the energy levels of the highest occupied molecular orbital (HOMO). The cyclic voltammograms of all three **Si3T** polymers are depicted in Figure S7 and summarized in Table 2.

Table 2. Summary of optical properties and frontier energy levels of **Si3T** polymers

Polymer	λ_{max}[a] [nm]	λ_{max}[b] [nm]	HOMO / LUMO[c] [eV]	E_g[d] [eV]
Si3T-BT	678	696	-5.0 (-4.46) / -3.5 (-2.48)	1.5 (1.98)
Si3T-FBT	691, 740	698, 756	-5.2 (-4.47) / -3.7 (-2.49)	1.5 (1.98)
Si3T-2FBT	680, 737	686, 746	-5.3 (-4.56) / -3.8 (-2.55)	1.5 (2.01)

[a] Dilute CB solution. [b] Thin film spin-casted from CB solution (5 mg/ml). [c] LUMO energy level estimated by adding the absorption onset to the HOMO energy level which was measured by cyclic voltammetry. Numbers in parentheses are calculated values determined via DFT calculations ((B3LYP/6-31G*) [d] Optical bandgap estimated form the UV-vis. absorption onset in solid state.

The effect of polymer backbone fluorination on the frontier energy levels is clearly apparent from the cyclic voltammetry data. The ionisation potential (IP) is gradually lowered with increasing fluorination. For **Si3T-BT** the IP was measured to be -5.0 eV, but significantly lowered by 0.2 eV in case of **Si3T-FBT**. Not surprisingly, the lowest IP was therefore measured for **Si3T-2FBT** at -5.3 eV. At the same time fluorine substituents are known to increase the electron affinity (EA), thus leading to constant bandgaps of 1.5 eV for all three polymers.[17, 18] The experimental observations are in good agreement with the theoretical calculations, summarized in Table 2. For all three **Si3T** polymers the LUMO wave functions are predominantly located on the BT moieties, as depicted in **Figure 3**.

Consequently the LUMO energy levels will be significantly influenced by any substituent on the BT unit, which translates into identical calculated bandgaps of 2 eV for all three polymers.

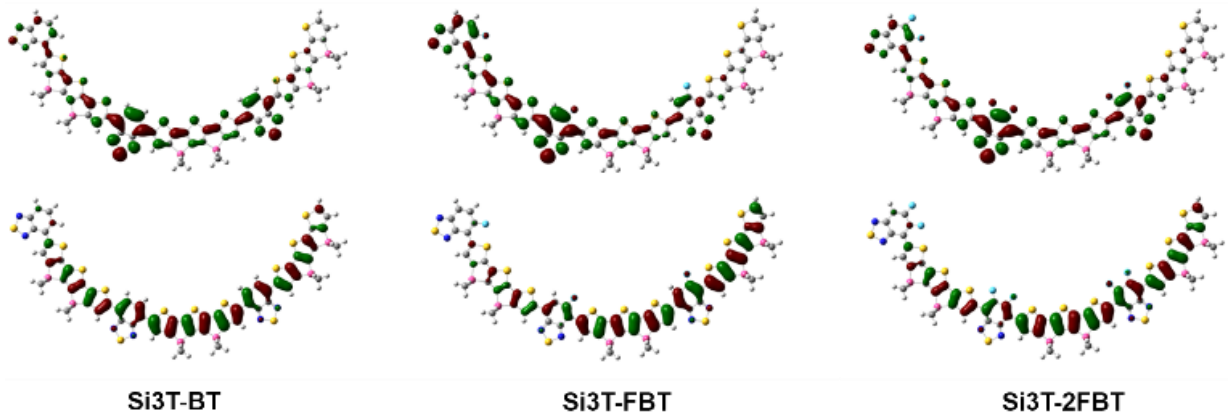

Figure 3. Energy-minimized structures (B3LYP/6-31G*) of methyl-substituted **Si3T** trimers with visualization of the HOMO (bottom row) and LUMO (top row) wave functions.

Density functional theory calculations on polymer trimers were performed at the B3LYP/6-31G* level of the theory to elucidate the polymer backbone curvature and the frontier wave function distributions (**Figure 3**). The curved shape of the **Si3T** donor unit with an angle of 117° introduces a backbone curvature into all three synthesized polymers. Previous reports revealed that extreme backbone curvatures can limit charge transport along the conjugated backbone, but at the same time Müllen *et al.* showed that a trade-off between charge carrier mobility and enhanced polymer solubility can be achieved with monomer angles around 120-130°.[19, 20] The HOMO wave functions are well delocalised along the polymer backbones, independent of the degree of fluorination on the benzothiadiazole

acceptor. The LUMO wave functions however are mainly localised on the acceptor parts in the polymer backbone.

The particular geometry of the pentacyclic **Si3T** monomer allows for the attachment of all four solubilising octyl chains on the same side of the aromatic core, thus reducing the steric hindrance on the opposite side, which has the potential to lead to improved molecular packing in solid state. To verify this hypothesis we recorded the x-ray diffraction (XRD) spectra of all three polymers and carried out differential scanning calorimetry (DSC) experiments to get a better understanding of the polymers solid state behaviour.

Before thermal annealing all polymer films form rather amorphous films with extremely weak and broad diffraction peaks at around 5.7°, associated to poorly ordered lamellar stacking of around 15.4 Å in distance (**Figure 4**). However after thermal annealing the crystallinity of the fluorinated polymers **Si3T-FBT** and **Si3T-2FBT** is significantly improved, whereas no change in diffraction pattern is observed for **Si3T-BT**. The monofluorinated polymer **Si3T-FBT** presents the sharpest (FWHM=0.23) and most intense diffraction peaks at 4.7°, corresponding to a lamellar stacking distance of 18.6 Å. The (100) diffraction peak of **Si3T-2FBT** at 4.7° (18.6 Å) is weaker in intensity and less well defined (FWHM=0.78), suggesting that the substitution of a second fluorine atom on the benzothidiazole, and subsequently less flexible backbone, renders the intermolecular chain organisation more difficult, leading to less crystalline films. Both fluorinated polymers also show weak diffraction peaks at higher 2θ values, caused by interchain π-π stacking distances of 3.6 Å.

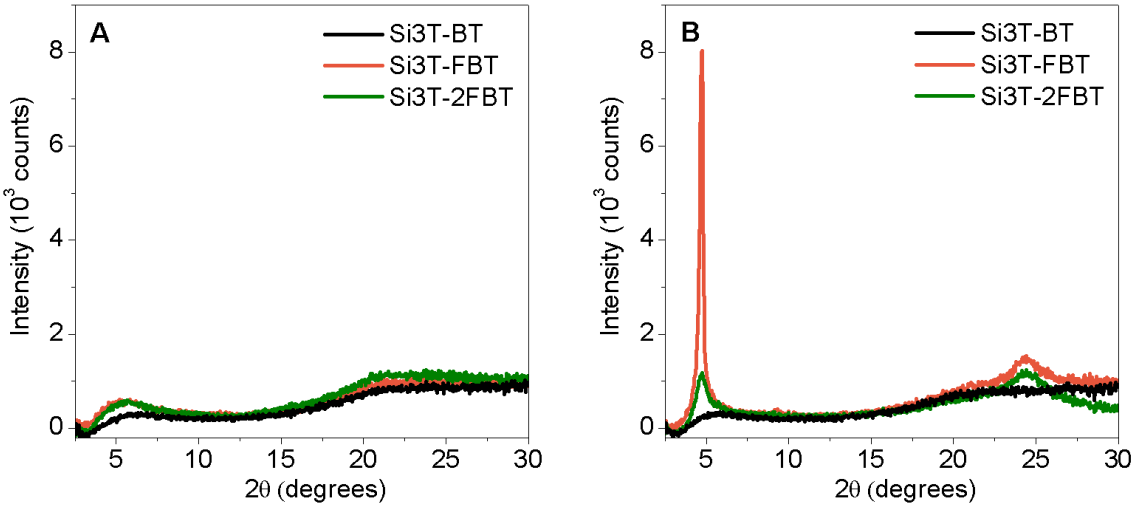

Figure 4. X-ray diffraction (XRD) patterns of **Si3T** polymer films drop-casted on silicon substrate from chlorobenzene (10 mg/mL), (A) as-cast film, (B) after annealing at 180°C for 10 minutes.

Comparing the XRD spectrum of **Si3T-2FBT** to the diffraction pattern of the previously published **Si4T-2FBT** it becomes apparent that attaching the alkyl chains on the same side of the fused building block instead of both sides, have a significant effect on the crystallinity of the polymers (See Supporting Information Figure S8).[7] Compared to the **Si3T** polymer, the **Si4T** polymer shows already some signs of crystallinity in the (100) plane prior to thermal annealing and even more so after thermal treatment. Moreover, the lamellar stacking distance of **Si3T-2FBT** is larger (18.6 Å) compared to 15.3 Å measured for the **Si4T-2FBT** polymer. We speculate that the curved backbone structure of the **Si3T** polymer leads to an increase in the lamellar stacking distance because dense packing of the alkyl chains is hindered by the backbone geometry. Interestingly a different trend is observed in the (010) plane, where the π-π stacking distances are shorter in the **Si3T** polymer then for

the **Si4T** polymer. The shorter π-π stacking distances are made possible by attaching the sterically hindering side chains on the same side of the fused monomer, thus making the pi-orbitals of the conjugated system more accessible for π-π interactions with adjacent polymer chains. At the same time however, ordered lamellar stacking is made more difficult because of the asymmetry of the **Si3T** monomer and the inhomogeneous distribution of alkyl side chains along the conjugated backbone.

DSC experiments were performed on all three **Si3T** polymers (See Supporting Information Figure S9 to S11), but did not deliver any further insight on the molecular packing due to the absence of phase transition peaks in the investigated temperature range (65 - 325°C).

All three **Si3T** based polymers were tested under simulated 100 mW cm^{-2} AM1.5G illumination in BHJ solar cells using a conventional device architecture consisting of ITO/PEDOT:PSS/polymer:$PC_{71}BM$/Ca/Al. The J-V curves are represented in **Figure 4** and key photovoltaic parameters are summarized in Table 3.

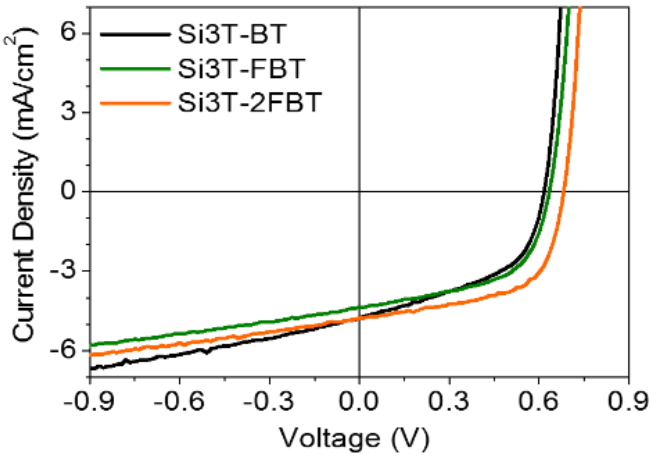

Figure 4. J-V curves of **Si3T**-polymer:$PC_{71}BM$ OPV devices.

As expected, the open-circuit voltage increases gradually from 0.62 V to 0.68 V with increasing backbone fluorination (corresponding to lowering the HOMO energy level) from **Si3T-BT** to **Si3T-2FBT**. The highest power conversion efficiency (PCE) of just under 2% was achieved with **Si3T-2FBT**. The device performances of all three polymers however are significantly limited by rather low short-circuit currents. AFM was used to investigate the active layer blend microstructure.

Table 3. Photovoltaic properties of the **Si3T** polymers

Polymer	J_{SC} [mA/cm^2]	V_{OC} [V]	FF	PCE [%]
Si3T-BT	4.76	0.62	0.48	1.4
Si3T-FBT	4.37	0.63	0.55	1.5
Si3T-2FBT	4.77	0.68	0.60	1.9

Conventional device architecture ITO/PEDOT:PSS/polymer:$PC_{71}BM$/ Ca/Al with a polymer:$PC_{71}BM$ blend ratio of 1:3 processed from *o*-dichlorobenzene.

The AFM micrographs in **Figure 5** suggest that the modest PCE values are related to poor bulk heterojunction morphologies and film quality. **Si3T-BT** has a finely dispersed polymer:$PC_{71}BM$ phase separation, however the film has a high concentration of pinholes, likely caused by poor substrate wetting due to the relatively low polymer molecular weight. With increasing fluorination of the polymer backbone however the phase separation dramatically increases and the formation of large domains (> 500 nm) is observed in the blend films of **Si3T-FBT** and **Si3T-2FBT**. Similar globular features have been previously observed in other polymer:fullerene blends and correlated to liquid-liquid phase separation during the film deposition process.[21, 22] The coarsened morphology in the fluorinated

polymers is likely to hinder efficient charge extraction from the active layer, resulting in the observed low photocurrents.

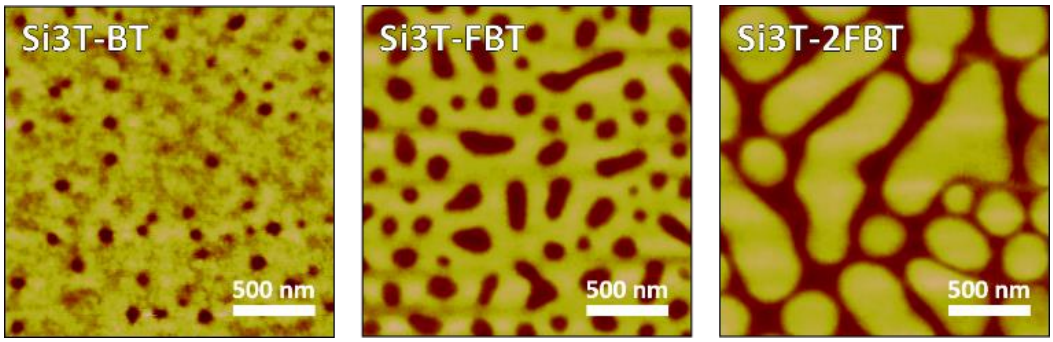

Figure 5. 2 × 2 μm AFM micrographs (tapping-mode) of **Si3T**-polymer:$PC_{71}BM$ (1:3) blends.

CONCLUSION

We demonstrated the synthesis of a new polyfused pentacyclic donor, whose geometry allows the single sided attachment of solubilizing alkyl side chains on the fused ring system. The new monomer was successfully introduced into a series of low bandgap donor polymers. The electronic properties of the resulting polymers could be gradually modified by increasing the fluorination along the polymer backbone. Besides the effect on the electronic structure, fluorination also proved a useful synthetic strategy to influence the crystallinity of the polymers in solid state. Even though the new **Si3T** donor polymers possessed promising electronic and optical properties, organic solar cells comprising these new materials did not achieve comparably high PCE's to the previously published **Si4T** polymers. AFM studies revealed that the observed low J_{sc} values are most likely the result of poor blend morphologies that prevent efficient charge extraction form the active layer.

ASSOCIATED CONTENT

Supporting Information. Synthetic procedures, polymer NMR spectra, cyclic voltammograms, UV-vis. absorption spectra, XRD data and additional AFM images. This material is available free of charge via the Internet at http://pubs.acs.org.

AUTHOR INFORMATION

Corresponding Author

* bschroeder@stanford.edu

Author Contributions

The manuscript was written through contributions of all authors. All authors have given approval to the final version of the manuscript.

ACKNOWLEDGMENT

BCS acknowledges the National Research Fund of Luxembourg for financial support. This work was in part carried out under the EPSRC Projects EP/F056710/1, EP/I019278/1 and EP/G037515/1 with support from the Centre for Plastic Electronics at Imperial College.

REFERENCES

1. Liang, Y.; Xu, Z.; Xia, J.; Tsai, S.-T.; Wu, Y.; Li, G.; Ray, C.; Yu, L. *Advanced Materials* **2010,** 22, (20), E135-E138.
2. Lu, L.; Yu, L. *Advanced Materials* **2014,** 26, (26), 4413-4430.
3. Schroeder, B. C.; Nielsen, C. B.; Kim, Y. J.; Smith, J.; Huang, Z.; Durrant, J.; Watkins, S. E.; Song, K.; Anthopoulos, T. D.; McCulloch, I. *Chemistry of Materials* **2011,** 23, (17), 4025-4031.
4. Nielsen, C. B.; Ashraf, R. S.; Treat, N. D.; Schroeder, B. C.; Donaghey, J. E.; White, A. J. P.; Stingelin, N.; McCulloch, I. *Advanced Materials* **2015,** 27, (5), 948-953.
5. McCulloch, I.; Ashraf, R. S.; Biniek, L.; Bronstein, H.; Combe, C.; Donaghey, J. E.; James, D. I.; Nielsen, C. B.; Schroeder, B. C.; Zhang, W. *Accounts of Chemical Research* **2012,** 45, (5), 714-722.

6. Venkateshvaran, D.; Nikolka, M.; Sadhanala, A.; Lemaur, V.; Zelazny, M.; Kepa, M.; Hurhangee, M.; Kronemeijer, A. J.; Pecunia, V.; Nasrallah, I.; Romanov, I.; Broch, K.; McCulloch, I.; Emin, D.; Olivier, Y.; Cornil, J.; Beljonne, D.; Sirringhaus, H. *Nature* **2014,** 515, (7527), 384-388.
7. Schroeder, B. C.; Ashraf, R. S.; Thomas, S.; White, A. J. P.; Biniek, L.; Nielsen, C. B.; Zhang, W.; Huang, Z.; Tuladhar, P. S.; Watkins, S. E.; Anthopoulos, T. D.; Durrant, J. R.; McCulloch, I. *Chemical Communications* **2012,** 48, (62), 7699-7701.
8. Graham, K. R.; Cabanetos, C.; Jahnke, J. P.; Idso, M. N.; El Labban, A.; Ngongang Ndjawa, G. O.; Heumueller, T.; Vandewal, K.; Salleo, A.; Chmelka, B. F.; Amassian, A.; Beaujuge, P. M.; McGehee, M. D. *Journal of the American Chemical Society* **2014,** 136, (27), 9608-9618.
9. Kanai, Y.; Wu, Z.; Grossman, J. C. *Journal of Materials Chemistry* **2010,** 20, (6), 1053-1061.
10. Marchiori, C. F. N.; Koehler, M. *Synthetic Metals* **2010,** 160, (7), 643-650.
11. Mitsudo, K.; Shimohara, S.; Mizoguchi, J.; Mandai, H.; Suga, S. *Organic Letters* **2012,** 14, (11), 2702-2705.
12. Ashraf, R. S.; Chen, Z.; Leem, D. S.; Bronstein, H.; Zhang, W.; Schroeder, B.; Geerts, Y.; Smith, J.; Watkins, S.; Anthopoulos, T. D.; Sirringhaus, H.; de Mello, J. C.; Heeney, M.; McCulloch, I. *Chemistry of Materials* **2010,** 23, (3), 768-770.
13. Nielsen, K. T.; Spanggaard, H.; Krebs, F. C. *Macromolecules* **2005,** 38, (4), 1180-1189.
14. Jackson, N. E.; Savoie, B. M.; Kohlstedt, K. L.; Olvera de la Cruz, M.; Schatz, G. C.; Chen, L. X.; Ratner, M. A. *Journal of the American Chemical Society* **2013,** 135, (28), 10475-10483.
15. Bronstein, H.; Frost, J. M.; Hadipour, A.; Kim, Y.; Nielsen, C. B.; Ashraf, R. S.; Rand, B. P.; Watkins, S.; McCulloch, I. *Chemistry of Materials* **2013,** 25, (3), 277-285.
16. Nielsen, C. B.; White, A. J. P.; McCulloch, I. *Journal of Organic Chemisrty* **2015**, 80, (10), 5045-5048.
17. Zhang, Y.; Chien, S.-C.; Chen, K.-S.; Yip, H.-L.; Sun, Y.; Davies, J. A.; Chen, F.-C.; Jen, A. K. Y. *Chemical Communications* **2011,** 47, (39), 11026-11028.
18. Fei, Z.; Shahid, M.; Yaacobi-Gross, N.; Rossbauer, S.; Zhong, H.; Watkins, S. E.; Anthopoulos, T. D.; Heeney, M. *Chemical Communications* **2012,** 48, (90), 11130-11132.
19. Rieger, R.; Beckmann, D.; Mavrinskiy, A.; Kastler, M.; Müllen, K. *Chemistry of Materials* **2010,** 22, (18), 5314-5318.
20. Lei, T.; Cao, Y.; Zhou, X.; Peng, Y.; Bian, J.; Pei, J. *Chemistry of Materials* **2012,** 24, (10), 1762-1770.
21. Kouijzer, S.; Michels, J. J.; van den Berg, M.; Gevaerts, V. S.; Turbiez, M.; Wienk, M. M.; Janssen, R. A. J. *Journal of the American Chemical Society* **2013,** 135, (32), 12057-12067.
22. van Franeker, J. J.; Westhoff, D.; Turbiez, M.; Wienk, M. M.; Schmidt, V.; Janssen, R. A. J. *Advanced Functional Materials* **2015,** 25, (6), 855-863.

TABLE OF CONTENTS

Dithienosilolothiophene, a new polyfused donor for organic electronics

*Bob C. Schroeder,[a, b, *] Mindaugas Kirkus,[a, c] Christian B. Nielsen,[a] Raja Shahid Ashraf,[a] and Iain McCulloch [a, c]*